ARTICLES

Electron Transfer to SF_6 and Oriented CH_3Br

Sean A. Harris, Susan D. Wiediger, and Philip R. Brooks*

Chemistry Department and Rice Quantum Institute, Rice University, Houston, Texas 77251

Received: June 15, 1999; In Final Form: July 26, 1999

Previous experiments have suggested that different negative ions are formed by electron transfer to different ends of a molecule. To investigate this possibility, a crossed molecular beam apparatus has been constructed to mass-analyze the ions produced in collisions between fast K atoms and oriented molecules. Initial studies are reported on ion formation in collisions of unoriented SF_6 and oriented CH_3Br. For lab energies $\approx$ 5−30 eV, Br^- is the only ion observed from CH_3Br, and its formation is favored by attack at the Br-end of CH_3Br. The Br and CH_3 ends have the same energetic threshold for forming Br^-. SF_5^-, SF_6^-, and F^- ions are observed from SF_6 and O_2^- from O_2. These ions are formed over a range of energies unlike those formed by electron attachment and suggest that the nascent negative ion can be stabilized by the accompanying positive K^+.

I. Introduction

Steric considerations are an ingrained aspect of chemical thought and a number of experiments have recently directly probed the role of orientation in chemical reaction.[1−9] These effects seem to be especially significant in electron transfer between initially neutral species as shown by Xing et al.[10,11] In these experiments, positive ions were observed from collisions between neutral potassium atoms and CF_3Br molecules which had been oriented in space. Attack at the Br-end of the molecule produced more positive ions than at the CF_3-end. The energetic threshold for the Br-end was $\approx$ 0.7 eV lower than for the CF_3-end, suggesting that attack at different ends of the molecule produced different negative ions.

These electron-transfer experiments exemplify the harpoon mechanism of Magee, et al.[12] in which an electron is transferred from an alkali metal atom to a halogen-containing molecule to form a transient ion-pair, which may then further interact to form neutral products. (Considerable evidence supports this mechanism, the most direct being the present observations that *ions* are formed if enough energy is available to separate the charges.[12−14]) Transient negative ions are formed in many other chemical reactions, especially those in solution, the most obvious examples being those in electrochemical cells.

How is the electron transferred? Ever since the days of J. J. Thompson,[15] the interaction of electrons with matter has been of enormous practical and theoretical interest.[16] Although both positive and negative ions can be formed by electron impact in the gas phase, attention has been mostly focused on positive ions since they are more robust and more convenient to handle. Any negative ions formed by electron attachment are inherently unstable because the total energy is above the dissociation limit to a free electron plus neutral atom or molecule. Even if a stable molecular ion exists, the Franck−Condon principle requires the nascent negative ion to be formed with the geometry of the neutral, which usually corresponds to the repulsive wall of the negative ion potential. Such a negative ion is thus most likely to autodetach (reform the electron and neutral) although molecular negative ions can dissipate energy by breaking chemical bonds to give radical negative ions.

In contrast to the gas phase, molecular negative ions are found in condensed phases because the solvent can deactivate the excited anion, and these anions play an important role in many chemical and biological electron-transfer processes. While it might thus seem that gas-phase (or molecular beam phase) experiments would be useless in addressing some issues in electron transfer, negative ions formed in atomic collision between neutrals are *different* from the negative ions formed by electron bombardment. Los and co-workers, for example, modeled ion formation in collision with alkali metal donors; they concluded that during the collision, "bond stretching" in the nascent molecular negative ion occurred due to the proximity of the positive alkali metal ion.[17] This stretching allowed the negative ion to more closely assume the geometry of the stable negative ion, and the electron affinity measured corresponded to the adiabatic (thermodynamic) electron affinity, being the difference in energy between the neutral in its ground-state geometry and the energy of the ion in its ground-state geometry. In contrast, electron attachment measures the vertical electron affinity, the energy difference between the neutral and negative ion with *both* in the geometry of the neutral. (This is likely to be negative; a vertical transition with the geometry of the neutral would usually lead to a repulsive portion of the anion potential.)

Formation of negative ions during collision, even during gas-phase collisions, is thus a potential tool for exploring molecular negative ions found in solution. To investigate the possibility of electron transfer being site specific, our oriented molecule apparatus has been modified to identify the ionic products in collisions between fast alkali metal atoms and oriented molecules. Methyl bromide is oriented, and SF_6 is used as a calibrant because it is spherically symmetric and has no mass combinations in common with CH_3Br. These collisions were expected

* Author to whom correspondence should be addressed.

10.1021/jp9919664 CCC: $18.00
Published on Web 08/31/1999

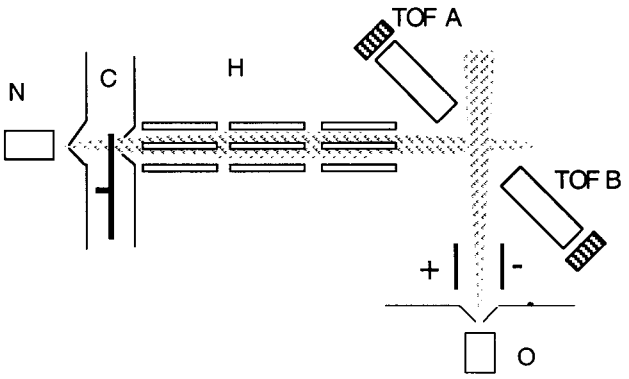

Figure 1. Schematic diagram of apparatus. A seeded supersonic beam emerges from nozzle N, passes through a skimmer for collimation, and can be modulated by chopper C. An inhomogeneous hexapole electric field H passes molecules in |JKM> states with KM < 0. These molecules are oriented in a uniform field. The oriented beam is crossed by a beam of fast K atoms formed in a charge-exchange oven O. An electrostatic field removes any ions from the alkali beam and the collisions studied are between neutral species. One time-of-flight detector detects positive ions, and the other negative ions. The potentials on the TOF detectors can be swapped to reverse the direction of orientation of the molecules.

to be different from those of free electrons (or Rydberg electrons), and that expectation is confirmed: the nascent alkali metal ion acts as a solvent to deactivate the nascent negative ion.[18] The only negative ion observed for CH_3Br is Br^-, and this is preferentially formed by Br-end attack.

II. Experimental Section

The apparatus shown in Figure 1 is a modification of that used earlier.[19,20] Neutral beams of oriented molecules are crossed with a beam of fast neutral potassium atoms. If the energy of the colliding pair is sufficiently high ($\approx$3−4 eV), an electron transfer creates a positive ion and negative ion which are detected in separate time-of-flight mass spectrometers. The mass spectrum can be obtained for attack of the K atom at the Br-end or CH_3-end of CH_3Br.

A. Oriented Molecules. A seeded (90% He) supersonic beam is passed through a 1400 mm hexapole electric field containing no apertures. Symmetric-top molecules with a permanent dipole moment, such as CH_3Br, have first-order Stark effects[21] and are deflected in an inhomogeneous electric field. In a hexapole electric field, molecules in |JKM> states are focused if KM < 0 and defocused if KM > 0, so the hexapole field acts as a filter which passes molecules in states with KM < 0. These molecules fly adiabatically into a region of uniform field $\approx$ 300 V/cm. Molecules in these selected states are *oriented* with respect to the direction of the weak field and the field direction can be reversed to present either the Br- or CH_3-end to the incoming beam of K atoms. The rotationally averaged orientation is $\langle \cos\theta \rangle = KM/(J(J+1))$ where θ is the average angle between the symmetry axis and the electric field. The quantum probability distribution for θ depends on J, K, and M. Even at rotational temperatures of a few K, several rotational states are still populated resulting in a distribution of orientations. This distribution is relatively monotonic[22] and can be thought of as an assembly of tops precessing about the field direction at various angles, θ. If the direction of the electric field is changed, the motion of the tops follows the field, keeping the same quantization with respect to the field, but changing directions in the laboratory. This distribution of orientations restricts our interrogation of the sample to "Br-end" vs "CH_3-end".

If no high voltage is applied, molecules pass through the hexapole without selection, and a weak, unselected, *and random* beam results. Likewise, no deflection or selection results for molecules without dipole moments, such as O_2 or SF_6, or for molecules without first-order Stark effects, such as CH_2Cl_2. For these molecules a weak but *random* beam also results.

B. Fast Alkali Atoms. Alkali metal atoms are produced with energies in the 0−30 eV range by surface ionizing atoms on a hot W filament, accelerating the ions by a voltage on a grid, and then allowing the ions to resonantly charge-exchange with the alkali gas as they pass through the oven.[23] Any residual ions in the beam are swept out by an external electric field, resulting in a beam containing only neutral species. The accelerating voltage is taken to be the nominal energy, and the well-known electron affinities for various SF_6 ions are used to calibrate the energy. Unfortunately, space charge effects greatly attenuate the beam at low energies, and very low count rates are observed near threshold.

C. Coincidence Time-of-Flight Mass Spectrometer. Ionizing collisions between the fast K atoms and the oriented molecules produce K^+ ions and M^- ions which are detected in separate time-of-flight (TOF) Wiley−McLaren[24] mass spectrometers. The molecular beams are continuous so the time zero and transit time through the mass spectrometer is unknown. But the ions are created simultaneously and the (unknown) time zero is the *same* for both ions. If the mass of the positive ion (almost certainly K^+) and the dimensions and voltages are known, then the time *difference* is a measure of the mass of the negative ion.

A schematic diagram of the mass spectrometer is shown in Figure 2. This design was inspired by those of Dunning and Meyer.[25,26] The orientation of the symmetric-top molecule at the reaction center is determined by the direction of the local electric field which needs to be parallel or antiparallel to the relative velocity. Ions formed in the collision will be extracted along the electric field, so the mass spectrometer array is rotated 25° with respect to the K beam to provide a field roughly parallel (antiparallel) with respect to the relative velocity. To reverse the orientation of the molecules, the direction of the electric field must be reversed, requiring reversal of the polarity of all of the electrodes which in turn reverses the direction the ions travel. A given TOF detector will thus collect positive ions in one orientation and negative ions in the other. The two TOF detectors are thus made identical.

Ions formed in the electron-transfer collision are accelerated toward their respective detectors by the electric field between the two TOF detectors. The ions then enter a field-free drift tube, and are deflected upward by a 45° electrostatic mirror into a second field-free region. The 57 mm diameter electrodes are spaced 6 mm apart with a 25 mm diameter opening. Elements in the mirror section are 2 mm apart. The positive ion and negative ion TOF sections are separated by 14.5 mm and the overall "drift tube" distance (triangular region of Figure 2 (right) + drift tube, D) is 128 mm. Grids are 95% transparent Ni mesh (Buckbee−Mears) and the ions are detected with Galileo microchannel plates with an active area 25 mm diameter. Typical operating voltages are $\pm$1450, $\pm$600, $\pm$600, and 0 for D, A, M1, and M2, giving a field strength in the collision region of about 300 V/cm. Relatively high potentials were used to minimize the loss of ions with appreciable transverse velocity components.

To avoid charge-up problems associated with oil contamination, the entire mass spectrometer assembly is contained in a UHV chamber pumped by a Varian triode ion pump. The beams

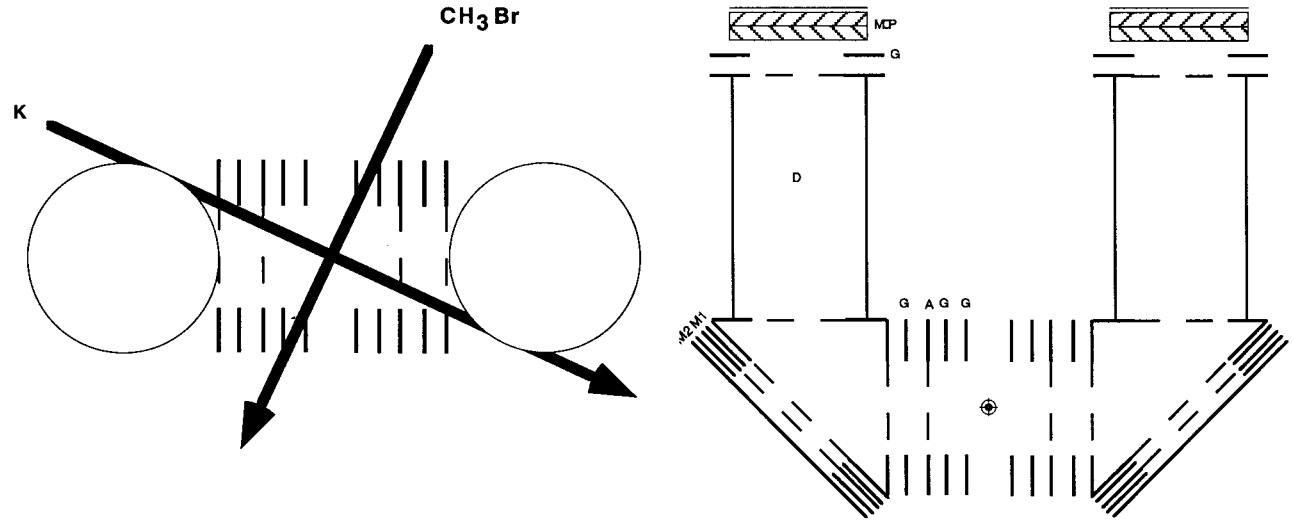

Figure 2. (left) Top view of dual TOF mass spectrometer. The mass spectrometer is rotated about the beam intersection by 25° so that the electric field is roughly parallel to the relative velocity vector. (right) Front view showing the beam intersection as a target, the ion mirror, and drift tube region. Ions are accelerated by potentials on the accelerator, A, and the drift tube, D, and reflected by the mirror M1 and M2. Intermediate potentials are placed on guard plates, G, to keep the field as uniform as possible. The beams, shown on left only, pass through holes cut in field plates and grids.

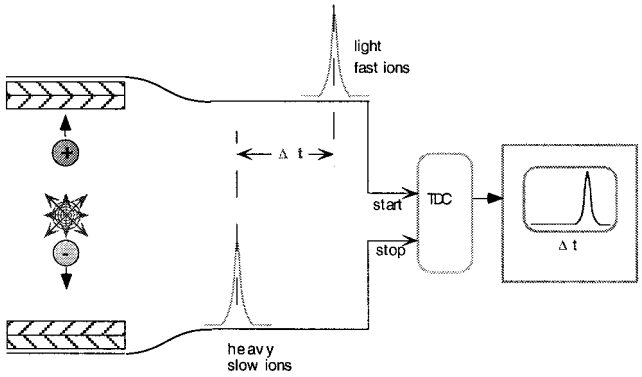

Figure 3. Principle of coincidence time-of-flight mass spectroscopy. Ions are created simultaneously by the electron transfer collision which occurs in an electric field serving not only to provide an axis for quantization but also to accelerate the ions. Positive and negative ions are drawn to their respective detectors. The flight distances and field strengths are equivalent for the two ions, so the lighter ion (the positive ion here) arrives at its detector first and starts a time-to-digital converter (TDC) The heavier ion arrives after a time Δt and stops the TDC which is then read by a computer. In practice, the negative ion pulse is always electronically delayed so that it provides the stop pulse.

enter and exit the UHV chamber through holes which can be sealed with mini-gate valves when the beams are not running. Operating pressures are typically in the high 10^{-8} Torr range.

The coincidence technique used here differs slightly from those more commonly used where the flight time of an ion is measured by starting a clock with an electron or photon. In the present experiments the positive and negative ions are of comparable mass and have comparable flight times. The positive and negative detectors must be identical so that polarities can be reversed to reverse the direction of orientation. The basic idea is sketched in Figure 3; the positive and negative ion are created simultaneously and have the same time zero. Each ion is accelerated to its respective detector, and the electronic pulse from the first ion to arrive is used to start a Lecroy 2228A time-to-digital converter (TDC) modified to have a full-scale range of 10 μs. The second ion stops the TDC and the time *difference*, Δt, is read by a computer. Since the positive ion is most likely K^+ in these experiments, Δt and the physical parameters (distances and voltages) determine the mass of the negative ion. For a molecule such as SF_6, a variety of different negative ions could be produced, such as e^-, F^-, SF_5^-, and SF_6^-, and in some cases the lightest ion is the negative ion. The negative ion pulse was delayed with a Stanford Research Systems digital delay generator in order to accommodate these possibilities.

III. Results

Mass Spectra. Different detectors with different efficiencies must be used for different orientations of a molecule. To compare signals from the different detectors, a small amount of a nonorientable gas (SF_6) is added to the CH_3Br/He gas mixture in the nozzle beam reservoir; typically SF_6:CH_3Br:He was 3%:7%:90%. Reaction of SF_6 is independent of the electric-field arrangement, and can be used to account for the different detection efficiencies, as well as different beam intensities on different days. Figure 4 shows typical coincidence time-of-flight spectra taken on different days for such a mixture with a 15.5 eV (lab) K atom beam. At these energies considerable fragmentation occurs in SF_6 and the ions SF_5^-, F^-, and SF_6^- are all observed. The only ion observed from CH_3Br is the Br^- ion. An O_2^- peak is from a small leak which was later sealed. A small number of electrons is observed from background collisions.

A difference in transit time is apparent for the two orientations, which can be understood from Figure 1. In the "straight-through" (ST) orientation, the K^+ ion is detected by TOF A, but in the "turn-around" (TA) orientation the positive ion is detected by TOF B. The initial velocity of the K atom is away from TOF B, and the K species must stop and turn around before heading to detector B. This makes the flight time for K^+ longer in the TA orientation, which can be seen in the arrival of the electron (which corresponds to a K^+, e^- *pair*). The heavier negative ion is less affected by the choice of detector A or B, and its travel time is roughly constant in the TA and ST orientations. The time difference between the K^+ and the heavier negative ions in the TA orientation is then smaller than in the ST orientation, as shown in Figure 4.

If the energy of the fast atom is zero or if the fast-atom beam is blocked, there are no coincidences. If the atomic beam is energized but the molecular beam is blocked, there are small coincidence signals arising from collisions of fast atoms with

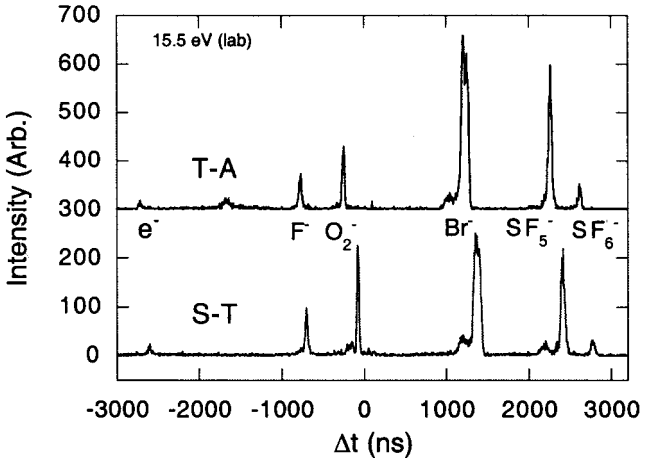

Figure 4. Coincidence TOF spectra for collisions of 15.5 eV K atoms with a CH_3Br/SF_6 beam. The clock is started by positive ion pulses and stopped by negative ion pulses delayed by 4 μs. Negative ions lighter than K^+ would arrive earlier than K^+ and are shown with negative Δt. TA and ST are "turn-around" and "straight-through" orientations discussed in the text. The spectra are normalized to have the same integrated SF_5^- signals, but distortion in the peaks requires that intensity comparisons be made from peak areas and not heights. (In this spectrum the Br^- intensity in the TA orientation is 1.3 times larger than in the ST orientation.)

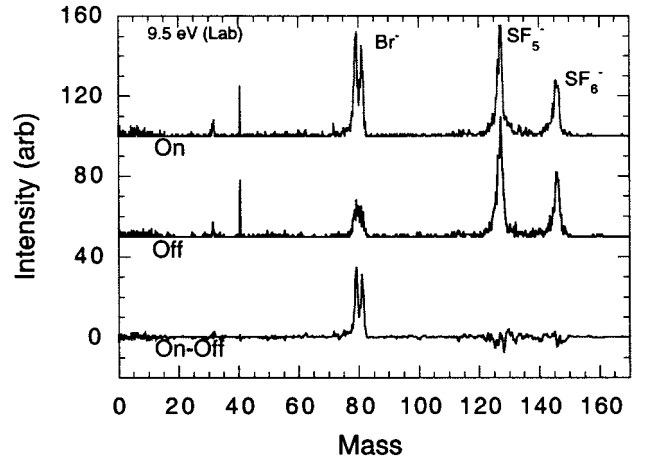

Figure 5. Coincidence TOF spectra for 9.5 eV (lab) K atoms colliding with a CH_3Br/SF_6 mixture in the turn-around orientation corresponding to attack at the Br end of CH_3Br. The top spectrum is taken with the high-voltage hexapole field on, the middle with the hexapole field off, and the bottom is the on−off difference showing the signal due only to oriented molecules.

background gases. These are discriminated against by taking data with the high-voltage hexapole field on and off, as illustrated in Figure 5. With the high voltage off, a weak unoriented beam of CH_3Br and SF_6 results in the middle spectrum. When high voltage is applied, the SF_6 intensity is unchanged, but the CH_3Br intensity increases because these molecules are focused and state-selected in the hexapole, and it is these molecules which are oriented. The difference is shown in the lowest spectrum. Signals from SF_6, unfocused CH_3Br and other background signals are subtracted out, and the result represents just the signal from the oriented molecules.

An enlargement of the Br^- peak from CH_3Br at 9.5 eV (lab) is shown in Figure 6 where splitting due to ^{79}Br and ^{81}Br is evident. A shoulder is also visible at lower mass which is due to the mass 41 isotope of K present to about 7% in the beam. The heavier ^{41}K isotope moves to the detector more slowly than ^{39}K, so Δt is smaller when the clock is started by ^{41}K and the

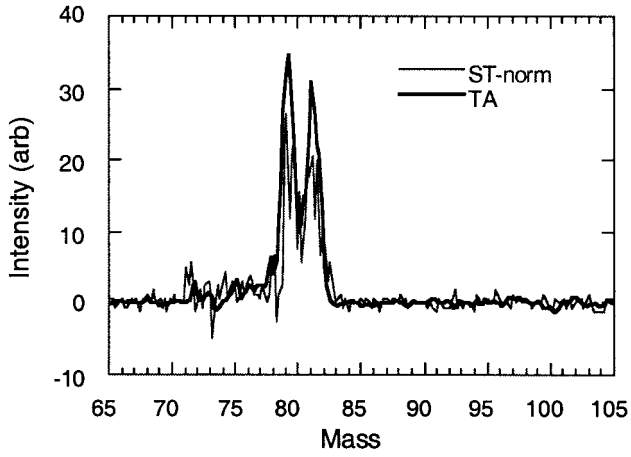

Figure 6. Enlargement of TOF mass spectrum showing Br^- intensities in the TA and ST orientations. The ST signals are normalized to make the SF_5^- reference signals equal for the two orientations. The TA signal is bigger and corresponds to attack at the Br-end of CH_3Br.

negative ion mass appears lighter. Similar shoulders are observed on other peaks. The mass scale is determined experimentally, but it agrees with electrostatic calculations to about 3%, which is the uncertainty in the voltages applied to the various electrodes.

Figure 6 also shows the effect of orientation on the production of Br^-. The signals from the straight-through (ST) orientation are normalized to make the SF_5^- signals the same in the two orientations. More Br^- ions are produced in the TA orientation, which corresponds to attack at the Br-end of the CH_3Br molecule.

Energy Dependence: SF_6. The most abundant ion in the energy range covered in these experiments is the fragment ion, SF_5^-, which is unambiguously identified because the mass is the same as that of I^- which we observe from CH_3I. Smaller amounts of SF_6^- and F^- are also observed. The experimental integrated intensity, $S^o_i(E)$, of a negative ion (i) at energy E for a specific orientation (o = ST or TA) is given by

$$S^o_i(E) = \sigma^o_i(E) I_K I_G D^\circ$$

where $\sigma^o_i(E)$ is the cross section for formation of ion i at energy E from orientation o, I_G is the intensity of the gas beam, I_K is the intensity of the K beam (which varies as $E^{3/2}$ because the source is space-charge limited[11,27]), and D° is a detector function which depends on orientation. The laboratory kinetic energy of the K atom is taken to be the accelerating voltage for the K^+ ions inside the charge exchange oven. The CM energy is $E_{CM} = 1/2\mu(v_K^2 + v_G^2)$ where μ is the reduced mass, $m_K m_G/(m_K + m_G)$, v and m are speed and mass, respectively, and subscripts G and K denote gas or K.

Unfortunately, neither the absolute intensities nor the detector function are known, and they are likely to vary from run to run. But for a specific gas mixture, the intensities of all ions are measured under the same conditions of beam intensity and detector function. Since D° is found to be roughly independent of energy, the unknown beam intensities and detector functions can be removed by defining the relative cross sections, $\sigma_i{}^o{}_R(E)$, relative to SF_5^- at 20 eV

$$\sigma_i{}^o{}_R(E) = \frac{S^o_i(E) 20^{3/2}}{S^o_{SF5}(20) E^{3/2}} \quad (1)$$

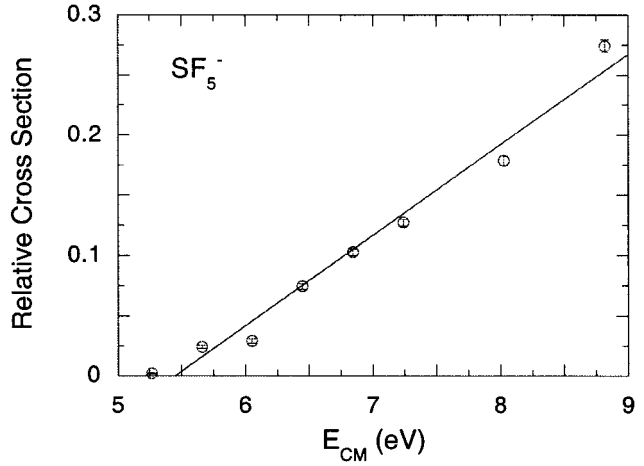

Figure 7. Relative cross section near threshold for formation of SF_5^- vs nominal CM energy. Error bars are $\pm 1\ \sigma$ calculated from Poisson statistics. The line is a linear least-squares fit.

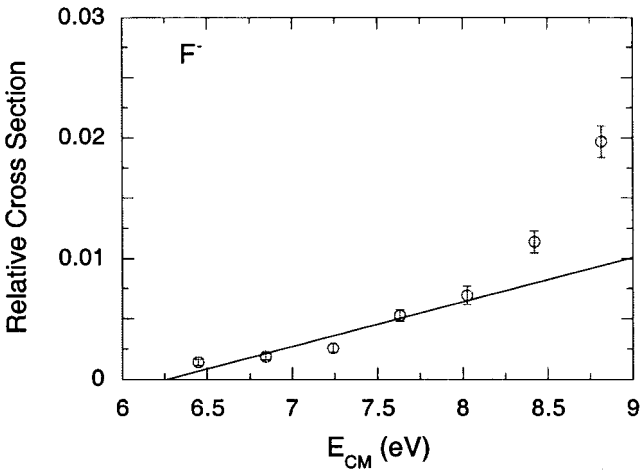

Figure 8. Relative cross section for formation of F^- vs nominal CM energy. Error bars are $\pm 1\ \sigma$ calculated from Poisson statistics. The line is a linear least-squares fit to the lowest few points.

Cross sections relative to SF_5^- at 20 eV (lab) are shown in Figures 7 − 10 for SF_5^-, F^-, SF_6^-, and Br^-, respectively. For the SF_6 species, the relative cross sections are calculated using the sum of ion intensities (HV-on + HV-off) averaged over the TA and ST "orientations".

Orientation of CH_3Br. The relative cross sections for Br^- produced in the TA and ST orientations are shown in Figure 10, where the data have again been normalized to the SF_5^- intensity at 20 eV in both the TA and ST configurations. For CH_3Br the relative cross sections shown in Figure 10 are the HV-on − HV-off *difference* illustrated in Figure 5.

The cross sections are clearly different, and depend on energy. To clearly emphasize the effect of orientation, we define the steric factor, *G*, as the cross section difference divided by the cross section sum,

$$G(E) = \frac{\sigma^{TA}_{Br}(E) - \sigma^{ST}_{Br}(E)}{\sigma^{TA}_{Br}(E) + \sigma^{ST}_{Br}(E)}$$

G is zero if there is no orientation difference, and G is one if only one end of the molecule is reactive. The steric factor for the formation of Br^- is plotted in Figure 11 and shows that the orientation becomes more important at low energies, with the Br-end of CH_3Br being favored by a factor of ≈2 at energies near 5 eV.

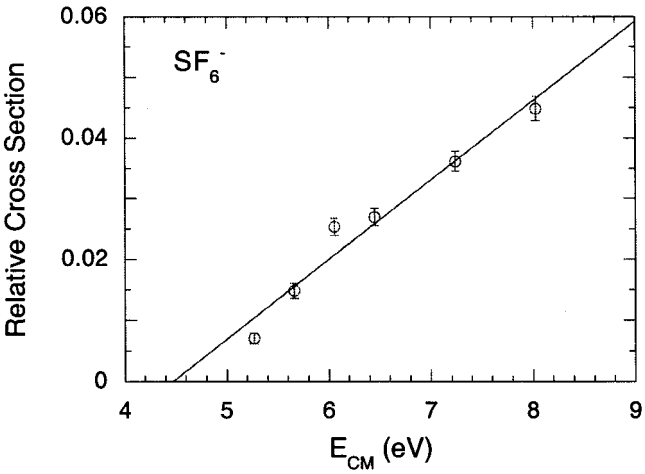

Figure 9. Relative cross section for formation of SF_6^- vs nominal CM energy. Error bars are $\pm 1\ \sigma$ calculated from Poisson statistics. The line is a linear least-squares fit.

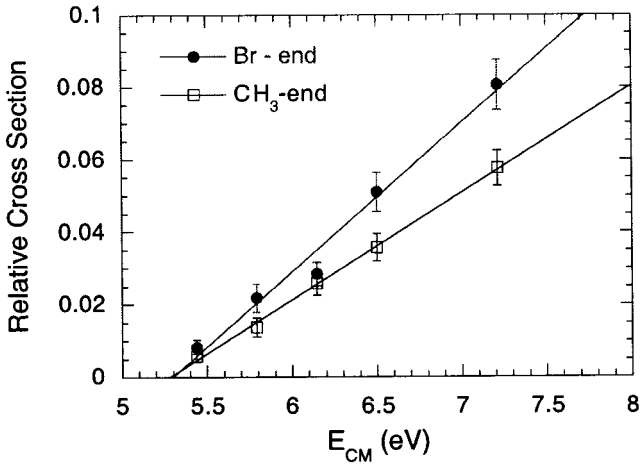

Figure 10. Relative cross section for production of K^+, Br^- ion-pairs from oriented CH_3Br vs nominal CM energy. Lines are least-squares fits and yield a common threshold of ≈5.3 eV.

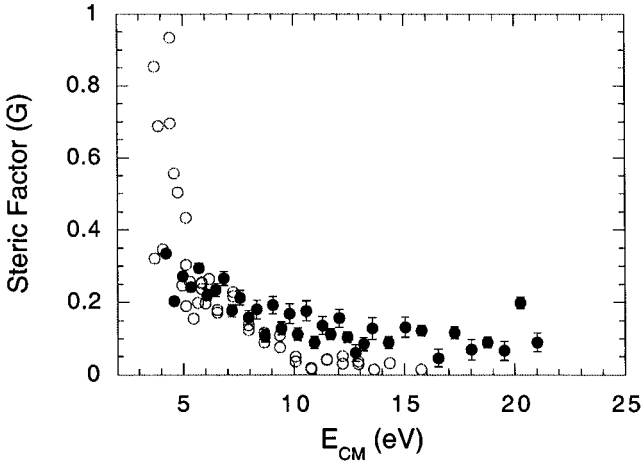

Figure 11. Steric factor *G* vs CM energy corrected using SF_6 ion thresholds. If reactivity were the same at both ends, $G = 0$; if only one end were reactive, *G* would be ±1, depending on the polarity of the oriented molecule. Open symbols are data of Xing [11] and refer to formation of all positive ions.

IV. Discussion

Ion Formation in SF_6. As anticipated, the dominant negative ion is SF_5^-, but SF_6^- is formed in appreciable amounts at collision energies as high as 20 eV. This is in agreement with

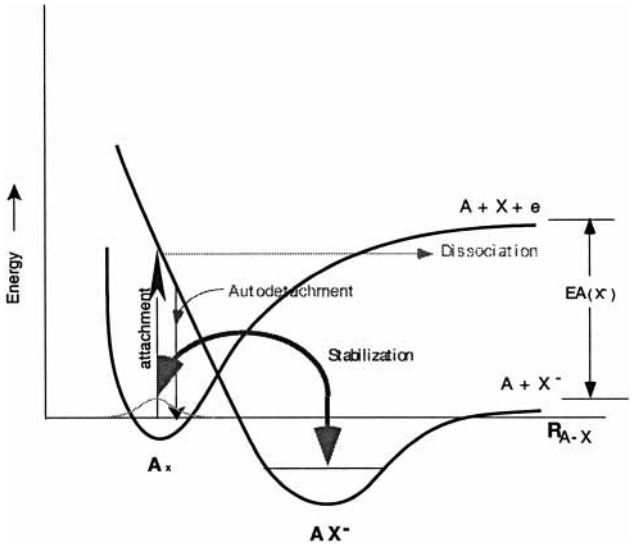

Figure 12. Schematic diagram of electron interactions with molecule AX. If AX^- is bound, it is likely to have a weaker and longer bond. Attachment of a free electron to AX will occur in a vertical, Franck−Condon like process in which the nuclei do not move, and AX^- will be formed in a state lying above the neutral molecule. This state is likely to rapidly autodetach the electron to reform the neutral plus electron, although it may also be stabilized by dissociation into fragments. The addition of a nearby positive ion core during electron attachment provides a "third body" which can stabilize the negative ion in a nonvertical process.

previous studies on collisional ionization[28−30] but in sharp contrast to studies with free electrons where conservation of energy requires that a negative ion be formed in a state lying above the autodetaching limit. Free electrons form *metastable* SF_6^-, but only from electrons with essentially zero kinetic energy.[31] At higher energies, electrons can be resonantly captured to form various fragment ions such as SF_5^- and F^-. In the present experiments these ions are formed over a wide range of energies, and they are formed from SF_6 which has been cooled in a supersonic expansion with a rotational temperature ≈ 4 K.[32]

Extensive studies with Rydberg atoms have shown that for large values of principal quantum number, *n*, Rydberg collisions are essentially collisions of "free" electrons.[33,34] This is understandable since the highly excited electron is far from the nucleus and is only barely bound; in short, the high Rydberg electron is essentially a free-electron. But deviations from free electron behavior are observed at "intermediate" values of n because these electrons are more tightly bound, the nucleus is closer, and the nucleus can interact with an incipient negative ion in a "post-attachment interaction."[35,36]

The collisions of ground-state atoms in the present work represents the limiting behavior of low Rydberg atoms: the electron is not free, and the nucleus plays a profound role in the collision. In contrast to the attachment of a free electron, a collision with a ground-state atom can produce a negative ion by electron attachment and the nearby nucleus can almost simultaneously deactivate the excited negative ion. Thus, collisions at 20 eV can easily transfer an electron to SF_6, which can fragment to SF_5^- or be deactivated by interaction with the K^+ core to form SF_6^-. (Similar considerations apply to O_2; electron attachment to O_2 yields O^-, but as shown in Figure 4, we observe O_2^-, and not O^-. The molecular negative ion is stable against autodetachment in only the first few vibrational levels,[37] so the collision apparently produces an ion in a low-lying vibrational state.) Thus the SF_6^- observed in these experiments is greatly stabilized, and may well be stable, but the lifetime has not yet been determined. Very few free electrons are seen, and these small signals seem to be from background processes, suggesting that stabilization of the negative ion is favored over autodetachment. The degree of stabilization will probably depend on both the donor and acceptor, since electron affinities measured with fast Rb atoms for CO_2 clusters are believed not to be the adiabatic electron affinities suggesting incomplete relaxation of the cluster anions.[38]

TABLE 1[a]

	threshold (eV)		
	experimental		
ion	uncorrected	corrected	theoretical
SF_6^-	4.63 ± 0.19		3.29[b]
SF_5^-	5.41 ± 0.10		4.49[b]
F^-	6.26 ± 0.19		4.84[b]
Br− (CH3-end)	5.27 ± 0.03	4.05	4.06
Br− (Br-end)	5.29 ± 0.08	4.07	

[a] These values used for energy calibration. [b] Data: IP(K) = 4.34[40] eV; EA(Br, F, SF_6, SF_5) = 3.36,[41] 3.45,[41] 1.05,[42,43] 3.8[44]eV; BDE ($F-SF_5$, CH_3-Br) = 3.95,[45] 3.08.[45]

Energy Thresholds. The kinetic energy of the K atoms is assumed to be the accelerating potential for the K^+ ions in the charge-exchange oven. In Xing's earlier work the speed of the atoms was measured, and found to agree well with the nominal accelerating voltage. Unfortunately, subsequent modifications in the charge-exchange oven make this calibration suspect and the collision energy is calibrated using the thresholds for the various SF_6 ions.

The apparent thresholds for formation of various ions, taken from Figures 7−10 are shown in Table 1. The energy scale is calibrated by linear interpolation of the SF_6 ion thresholds, and the corrected Br^- threshold after calibration of the beam energy is 4.05 eV, in good agreement with the theoretical threshold calculated from ionization potentials, electron affinities, and bond dissociation energies. (The leak causing the O_2 impurity mentioned earlier was repaired before the lower energy scans were taken, and O_2 was unavailable as a calibrant.)

Steric Effects in CH_3Br. The only negative ion observed so far[39]from CH_3Br is Br^-. This ion is found to be more likely formed in the turn-around orientation where the positive ion detector is TOF B in Figure 1. Since the hexapole field selects molecules in states in which the energy increases with field, the negative end of the molecule points toward negatively biased detector B. In this orientation the negative end of the molecule is attacked, and we assume the negative end is the Br-end of the molecule.

The Br-end of the molecule is the more reactive end at all energies, and the Br-end is roughly twice as reactive as the CH_3-end at low energies. As shown in Figure 10, the Br-end and CH_3-end cross sections have the same apparent threshold. This might seem in contradiction to the earlier data of Xing which reported somewhat larger reactivity ratios and which suggested that the Br-end and CH_3-end *might* have different energetic thresholds.

But Xing detected only the positive ions formed in the collision. If a negative ion other than Br^- is formed this would have been included in Xing's experiments although it would not be included here. For example, if the parent negative molecular ion CH_3Br^- were formed, Xing might have measured its threshold in one orientation. (We have not observed CH_3Br^-, although we have independently observed the parent negative molecular ion CF_3Br^- and defer a detailed study to use a

calibrant other than SF_6.) The present (K^+, Br^-) coincidence signals do not include any contribution from other ions and show that although the signal depends on orientation and energy, the threshold is determined only by the energy, as is to be expected from thermodynamics.

V. Summary

Collisions of fast potassium atoms with SF_6 and CH_3Br produce ions which have been identified. Ions from SF_6 are different from those expected from electron impact and suggest that the nascent K^+ ion can play the role of a solvent and deactivate the nascent negative ion.

The CH_3Br molecule can be oriented prior to collision. More Br^- ions are formed when the Br-end of the molecule is attacked, but the energetic threshold is the same regardless of orientation.

Acknowledgment. We gratefully acknowledge financial support from the National Science Foundation and the Robert A. Welch Foundation. We have benefited from the previous experience in this lab gleaned by Howard Carman, Leon Phillips, Peter Harland, Guoqiang Xing, and Dock-Chil Che, and we thank them for their contributions. We thank Ken Smith and Mike Duncan for helpful discussions.

References and Notes

(1) Brooks, P. R. *Science* **1976**, *193*, 11.
(2) Loesch, H. J. *Annu. Rev. Phys. Chem.* **1995**, *46*, 555.
(3) Bernstein, R. B.; Herschbach, D. R.; Levine, R. D. *J. Phys. Chem.* **1987**, *91*, 5365.
(4) Slenczka, A.; Friedrich, B.; Herschbach, D. *Phys. Rev. Lett.* **1994**, *72*, 1806.
(5) Friedrich, B.; Pullman, D. P.; Herschbach, D. R. *J. Phys. Chem.* **1991**, *95*, 8118.
(6) Aitken, C. G.; Blunt, D. A.; Harland, P. W. *J. Chem. Phys.* **1994**, *101*, 11074.
(7) Bulthuis, J.; vanLeuken, J. J.; Stolte, S. *J. Chem. Soc., Faraday Trans.* **1995**, *91*, 205.
(8) Kuwata, K.; Kasai, T. *The Chemical Dynamics and Kinetics of Small Radicals*, Vol. II; Liu, K., Wagner, A., Eds.; World Scientific: Singapore, 1995; p 842.
(9) Brooks, P. R.; Harland, P. W. *Advances in Gas-Phase Ion Chemistry*, Vol. 2; Adams, N. G., Babcock, L. M., Eds.; JAI Press: Greenwich, CT, 1996; p 1.
(10) Xing, G.; Kasai, T.; Brooks, P. R. *J. Am. Chem. Soc.* **1994**, *116*, 7421.
(11) Xing, G.; Kasai, T.; Brooks, P. R. *J. Am. Chem. Soc.* **1995**, *117*, 2581.
(12) Baede, A. P. M. *Adv. Chem. Phys.* **1975**, *30*, 463.
(13) Lacmann, K. *Adv. Chem. Phys.* **1980**, *30*, 513.
(14) Los, J.; Kleyn, A. W. *Alkali Halide Vapors*; Davidovits, P., McFadden, D. L., Eds.; Academic Press: New York, 1979; p 279.
(15) Thompson, J. J. *Proc. R. Soc. (London)* **1913**, *89A*, 1.
(16) *Electron−Molecule Interactions and Their Applications*; Christophorou, L. G., Ed.; Academic Press: Orlando, FL, 1984.
(17) Aten, J. A.; Los, J. *Chem. Phys.* **1977**, *25*, 47.
(18) Nalley, S. J.; Compton, R. N.; Schweinler, H. C.; Anderson, V. E. *J. Chem. Phys.* **1973**, 4125.
(19) Wiediger, S. D. Ph.D. Thesis, Rice University, Houston, TX, 1998.
(20) Xing, G. Ph.D. Thesis, Rice University, Houston, TX, 1993.
(21) Townes, C. H.; Schawlow, A. L. *Microwave Spectroscopy*; Dover: New York, 1975.
(22) Brooks, P. R. *Int. Rev. Phys. Chem.* **1995**, *14*, 327.
(23) Helbing, R. K. B.; Rothe, E. M. *Rev. Sci. Instrum.* **1968**, *39*, 1948.
(24) Wiley, W. C.; McLaren, I. H. *Rev. Sci. Instrum.* **1955**, *26*, 1150.
(25) Kalamarides, A.; Walter, C. W.; Lindsay, B. G.; Smith, K. A.; Dunning, F. B. *J. Chem. Phys.* **1989**, *91*, 4411.
(26) Meyer, H. *J. Chem. Phys.* **1994**, *101*, 6697.
(27) Aten, J. A.; Los, J. *J. Phys. E* **1975**, *8*, 408.
(28) Compton, R. N.; Cooper, C. D. *J. Chem. Phys.* **1973**, *59*, 4140.
(29) Hubers, M. M.; Los, J. *Chem. Phys.* **1975**, *10*, 235.
(30) Leffert, C. B.; Tang, S. Y.; Rothe, E. W.; Cheng, T. C. *J. Chem. Phys.* **1974**, *61*, 4929(L).
(31) Fenzlaff, M.; Gerhard, R.; Illenberger, E. *J. Chem. Phys.* **1988**, *88*, 149.
(32) Wiediger, S. D.; Harland, P. W.; Holt, J. R.; Brooks, P. R. *J. Phys. Chem. A* **1998**, *102*, 1112.
(33) Zollars, B. G.; Higgs, C.; Lu, F.; Walter, C. W.; Gray, L. G.; Smith, K. A.; Dunning, F. B.; Stebbings, R. F. *Phys. Rev. A* **1985**, *32*, 3330.
(34) Dunning, F. B.; Stebbings, R. F. *Annu. Rev. Phys. Chem.* **1982**, *33*, 173.
(35) Zollars, B. G.; Walter, C. W.; Lu, F.; Johnson, C. B.; Smith, K. A.; Dunning, F. B. *J. Chem. Phys.* **1984**, *84*, 5589.
(36) Zheng, Z.; Smith, K. A.; Dunning, F. B. *J. Chem. Phys.* **1988**, *89*, 6295.
(37) Massey, H. S. W. *Negative Ions*; Cambridge University Press: New York, 1976.
(38) Quitevis, E. L.; Herschbach, D. R. *J. Phys. Chem.* **1989**, *93*, 1136.
(39) Compton, R. N.; Reinhardt, P. W.; Cooper, C. D. *J. Chem. Phys.* **1978**, *68*, 4360.
(40) Moore, C. E. *Atomic Energy Levels*, Vol. 467; National Bureau of Standards: Washington, DC, 1949.
(41) *Handbook of Chemistry and Physics*, 71 ed.; Lide, D. R., Ed.; CRC Press: Boca Raton, FL, 1990.
(42) Kebarle, P.; Chowdury, S. *Chem. Rev.* **1987**, *87*, 513.
(43) Chen, E. C. M.; Wiley, J. R.; Batten, C. F.; Wentworth, W. E. *J. Phys. Chem.* **1994**, *98*, 88.
(44) Chen, E. C. M.; Shuie, S.-R.; D'sa, E. D.; Batten, C. F.; Wentworth, W. E. *J. Chem. Phys.* **1988**, *88*, 4711.
(45) McMillen, D. F.; Golden, D. M. *Annu. Rev. Phys. Chem.* **1982**, *33*, 493.